Physics Letters B 786 (2018) 16–20

Contents lists available at ScienceDirect

Physics Letters B

www.elsevier.com/locate/physletb

Multi-messenger investigation of the Pygmy Dipole Resonance in ^{140}Ce

D. Savran [a,*], V. Derya [b], S. Bagchi [c,a], J. Endres [b], M.N. Harakeh [c], J. Isaak [d], N. Kalantar-Nayestanaki [c], E.G. Lanza [e], B. Löher [d], A. Najafi [c], S. Pascu [b,f], S.G. Pickstone [b], N. Pietralla [d], V.Yu. Ponomarev [d], C. Rigollet [c], C. Romig [d], M. Spieker [b], A. Vitturi [g,h], A. Zilges [b]

[a] GSI Helmholtzzentrum für Schwerionenforschung GmbH, Darmstadt, Germany
[b] Institut für Kernphysik, Universität zu Köln, Köln, Germany
[c] KVI-CART, University of Groningen, Groningen, the Netherlands
[d] Institut für Kernphysik, Technische Universität Darmstadt, Darmstadt, Germany
[e] INFN Sezione di Catania, Catania, Italy
[f] National Institute for Physics and Nuclear Engineering, Bucharest – Magurele, Romania
[g] Dipartimento di Fisica e Astronomia "Galileo Galilei", Universita di Padova, Italy
[h] INFN Sezione di Padova, Padova, Italy

ARTICLE INFO

Article history:
Received 21 July 2018
Received in revised form 31 August 2018
Accepted 13 September 2018
Available online 14 September 2018
Editor: V. Metag

Keywords:
Pygmy Dipole Resonance
E1 strength
Direct reactions
Collective levels
Quasi-particle Phonon Model

ABSTRACT

We report on the first $(p, p'\gamma)$ experiments at $E_p = 80$ MeV to investigate the Pygmy Dipole Resonance (PDR) in the semi-magic nucleus ^{140}Ce. This experiment is the latest in a series of experiments to investigate the PDR with different complementary probes to provide a multi-messenger data set on the properties of the PDR in ^{140}Ce. In addition, calculations within the Quasi-particle Phonon Model (QPM) have been performed. Cross sections have been calculated for proton- as well as α-scattering reactions based on the transition densities obtained from the QPM, not only at the RPA level, but including the full model space of up to 3p–3h configurations. This allows for the first time to compare the calculations to the experimental results on an absolute scale for single excitations. Agreement between QPM and experiment is observed, which proves the high accuracy of the calculated transition densities for individual PDR states.

The experimental investigation of the same phenomenon using different complementary observables can be the clue to understand its basic nature and to verify the theoretical modelling. A recent example in the field of astrophysics is the simultaneous observation of gravitational as well as electromagnetic signals from the same astrophysical event, which allowed to identify a binary neutron star merger followed by a γ-ray burst as the common source [1]. In this letter we present a multi-messenger investigation of a nuclear excitation mode, the so-called Pygmy Dipole Resonance [2,3], which is currently of high interest in the field of nuclear physics. Complementary observables are extracted from different experiments using a combination of hadronic and electromagnetic probes and are compared to corresponding results from a microscopic model calculation. This provides a comprehensive test of the quality of the theoretical model.

A microscopic understanding and experimental investigation of the PDR is not only interesting from a nuclear structure point of view but important for applications in related fields as well. The PDR and the low-lying E1 strength in general has consequences on reaction rates in nuclear astrophysics calculations of the synthesis of the heavy elements [4–7] due to its location at lower excitation energies. It is directly linked to radiative strength functions which are one of the main ingredients within the statistical model. Understanding the low-lying E1 strength in atomic nuclei is therefore important for the reliability of calculations making use of codes such as TALYS [8] or EMPIRE [9], which are for example also used in the design of the next-generation nuclear power plants [10] and the transmutation of nuclear waste [11,12]. Since the reactions in astrophysical scenarios often involve very neutron-rich (unstable) nuclei, where the PDR is expected to be strongly enhanced, a reliable extrapolation to exotic nuclei within microscopic calculations is needed. Therefore, an extensive test of various properties of the PDR in modern microscopic calculations is mandatory. Another aspect further stimulating the investigation of low-lying E1 strength

* Corresponding author.
E-mail address: d.savran@gsi.de (D. Savran).

https://doi.org/10.1016/j.physletb.2018.09.025

is its connection to isovector properties of the equation of state (EoS) of nuclear matter via the dipole polarisability [13–16]. Using this link, parameters in the asymmetry-dependent part of the EoS can be extracted, which are only insufficiently constrained by other experimental observables but are important to calculate for example the properties of neutron stars [17,18]. The connection of the E1 strength to the EoS is done within microscopic model calculations. A comprehensive test of microscopic models using multiple observables is therefore also important for this application.

A basic approach to study the structure of excitations is to investigate the response to external fields, i.e. scattering experiments in nuclear physics. In this letter we report on a systematic investigation of the PDR in ^{140}Ce using different probes, which allows to test various aspects of the wave functions of the involved excitations. The latest experiment uses the $(p, p'\gamma)$ reaction and is presented here for the first time. The experiments are accompanied by calculations within the Quasi-particle Phonon Model (QPM) [19]. Previously we have reported on the reproduction of the fragmentation of the E1 strength in QPM calculations [20,21]. In the present work we have used the transition densities from the QPM to calculate (α, α') as well as (p, p') inelastic scattering cross sections with the full set of excitations, thus allowing to compare the calculations with experiment on a quantitative level for the first time.

Experimentally, the PDR has mainly been studied by measuring the photo-absorption cross sections which is dominated by the electric dipole (E1) response of (spherical) nuclei, either by real-photon induced reactions [22–28,7,29] or Coulomb excitation in normal [30–32] and inverse [33–35] kinematics. The latter gives access to investigate the PDR in neutron rich unstable isotopes, such as ^{68}Ni, where recently the dipole polarisability has been measured [35]. For a more complete summary of available experimental results on the PDR see [2]. First experiments using a complementary probe to photons revealed a structural splitting of the low-lying E1 strength in a number of nuclei by the $(\alpha, \alpha'\gamma)$ reaction [36–41]. Combining these results with microscopic calculations has finally allowed to identify the structure of the low-lying part of the PDR as the oscillation of excess neutrons at the surface of the nucleus [42]. Experiments using the $(^{17}O, ^{17}O'\gamma)$ reaction have confirmed the observed splitting [43–46] recently. This shows how combining different experimental approaches helps to pin down the structure of nuclear excitations. In this letter, we present first $(p, p'\gamma)$ experiments at $E_p = 80$ MeV, which provides further experimental information on the PDR in ^{140}Ce.

The ^{140}Ce$(p, p'\gamma)$ experiment was performed at the KVI in Groningen, the Netherlands. The proton beam with an average current of 0.6 nA was delivered by the AGOR super-conducting K600 cyclotron. Protons with a kinetic energy of 80 MeV impinged on a highly enriched (99.72%) metallic ^{140}Ce target with a thickness of 20 mg/cm^2. The Big-Bite Spectrometer (BBS) [47] positioned at 5.6° relative to the beam axis was used in combination with the EuroSuperNova (ESN) detection system [48] for the detection of the scattered protons. Two parallel vertical-drift chambers (VDCs) are utilized to reconstruct the trajectories of the incoming particles. In addition, two plastic scintillator detectors are located behind the VDCs. The first scintillator detector is used as a particle trigger to implement the hardware coincidence between the BBS and the HPGe detectors which reduces the dead time of the system. A solid angle of 9.2 msr was covered by the spectrometer and the excitation energy resolution amounted to 217(1) keV at $E_x = 1.6$ MeV. The emitted γ-rays were detected by an array of eight HPGe detectors placed around the target chamber and providing in total a photo-peak efficiency of 0.467(7)% at 1.2 MeV. A more detailed description of the coincidence setup at the Big-Bite Spectrometer can be found in [49].

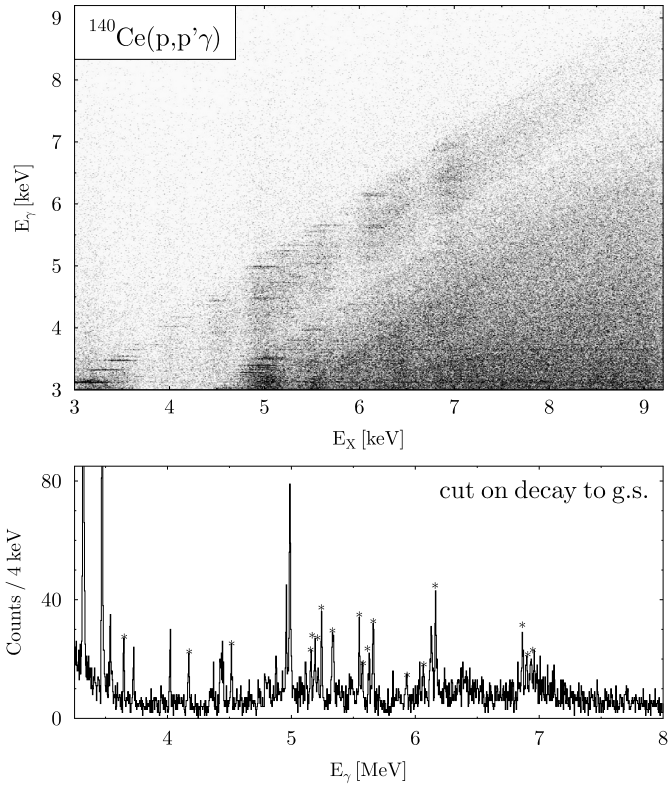

Fig. 1. Upper part: Two-dimensional spectrum showing the correlation between the measured proton energy loss (nuclear excitation energy) on the x-axis and the detected γ-ray energy on the y-axis. Transitions between nuclear states appear as thin horizontal lines, which are ordered in diagonal bands, each corresponding to the decay to a certain lower lying state. The uppermost band with $E_\gamma \approx E_X$ represents the decays back to the ground state. Lower part: Projected γ-ray spectrum with gate on ground-state transitions. Peaks marked with an asterisk can be assigned to 1^- states known from (γ, γ').

The acquired listmode data were sorted into p–γ coincidence matrices (see upper part of Fig. 1) containing the correlated information of the excitation energy (E_X) and γ-ray energy (E_γ). The nuclear excitation energy was determined by the energy loss of the scattered protons. We refer to the analogue technique used for $(\alpha, \alpha'\gamma)$ described in [37,39] for a detailed description of the single analysis steps and only give a brief outline here. Ground-state γ-ray transitions of excited states can be selected by setting energy gates, $E_x \approx E_\gamma$, for the projections on the axes. This selection yields a sensitivity to $J^\pi = 1^-$ excited states due to their allowed E1 transition to the ground state. The resulting projected γ-ray spectrum summed over all HPGe detectors is shown in the lower part of Fig. 1. The γ angular distribution is sensitive to the multipole character of the transition as shown in [37,39]. The statistics for single HPGe detectors in the present experiment was not sufficient for a quantitative analysis of the angular distribution in most cases. Thus, the identification is performed by the comparison to the Nuclear Resonance Fluorescence (NRF) data for which spin and parity have been determined unambiguously [50,51,28].

Excitation cross sections for the individual states are extracted from the intensities in the spectra by accounting for the p–γ angular correlation following the analysis presented in [37,39]. The same branching ratio Γ_0/Γ for the single states as in the analysis of the NRF experiments was taken into account ($\Gamma_0/\Gamma = 1$ in most cases). The resulting cross sections are shown in Fig. 2 together with the data from the previous experiments on ^{140}Ce and the results of the QPM calculations. Uncertainties of the present results are in the region of 10–20% in most cases.

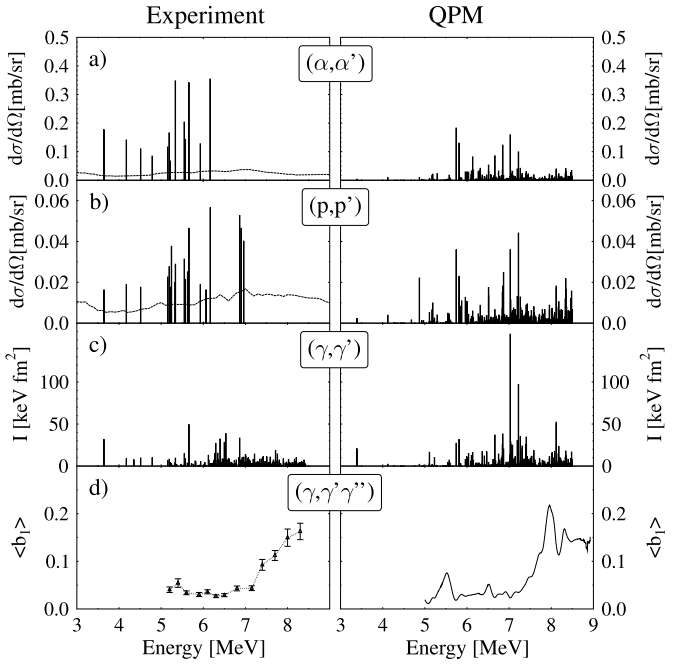

Fig. 2. The experimental results for the present $(p, p'\gamma)$ experiment are shown in panel b) together with the results for the previous experiments using the $(\alpha, \alpha'\gamma)$ [36] and the NRF reaction [52,53]. The solid lines in panel a) and b) represent the sensitivity limit of the experiments. The lowest panel shows the measured averaged branching ratio to the first excited state as published in [28]. In the right column, the corresponding calculations within the QPM model are shown. For more details see text.

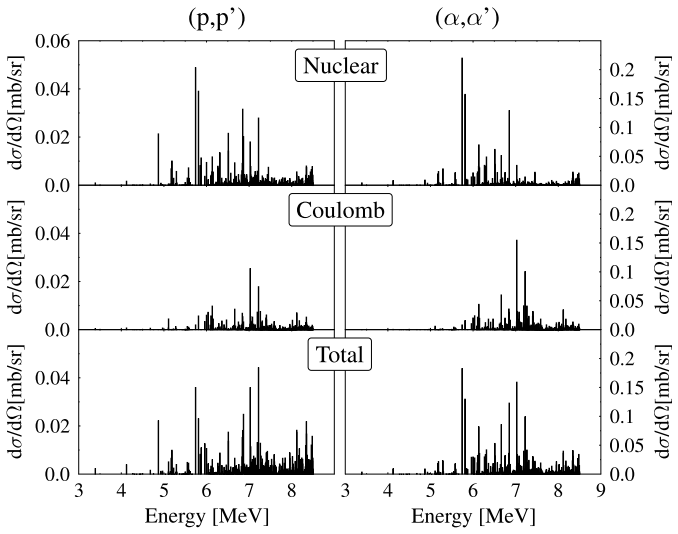

Fig. 3. Decomposition of the calculated cross sections for (p, p') and (α, α') into pure nuclear interaction, pure Coulomb interaction and total cross section including nuclear-Coulomb interference.

Calculations have been performed with the QPM wave functions from [21]. They have been obtained by diagonalization of the model Hamiltonian on the basis of interactive one-, two-, and three-phonon configurations. Two- and three-phonon configurations were built up from the phonons with the multipolarities from $1^{\pm}$ to $9^{\pm}$ and were cut above 8.5 MeV. In total we have 1157 1^- states below this energy cut. The ^{140}Ce(p, p') and ^{140}Ce(α, α') cross sections have been calculated for all of them.

The (p, p') cross sections have been computed within the DWBA (distorted-wave Born approximation) employing the DWBA07 code [54]. The effective NN-interaction of Love–Franey [55,56] has been used as input to calculate both the optical potential and transition amplitudes. The cross sections have been averaged over the scattering angle $\theta = 3.3°$–$7.9°$ in accordance with the acceptance angle of the BBS. They exhibit a smooth dependence on θ and drop by 35% from the smaller to the larger angle.

The (α, α') cross section have been calculated within a semi-classical coupled-channel model described in [57–59]. The radial form factors were calculated by a double folding procedure with the transition densities provided by the QPM and using a M3Y nucleon–nucleon (NN) interaction [60]. For the real part of the optical potential the double-folding procedure has been used with the QPM ground-state density for ^{140}Ce and the one given in [61] for the alpha particle. The imaginary part is taken with the same geometry of the real part with half of the strength. The cross sections are then obtained by integrating the inelastic probability amplitude for each dipole state over the range of impact parameters that lead to the scattered projectile in the measured angular range.

The mechanism of the electromagnetic excitation in the photoabsorption reaction is well known. For the excitation of 1^- states it is of isovector nature. Protons and α-particles interact with the target nuclei by means of the Coulomb- and NN-terms. The former is proportional to the electromagnetic transition. The latter is predominantly of isoscalar nature at the present kinematics in both (p, p') and (α, α') reactions, although some admixture of the isovector part is also present.

To investigate the role of the above-mentioned terms for the hadronic projectiles, the cross section calculations for both reactions have been repeated for each term separately. Corresponding results are presented in the upper two rows of Fig. 3 as "Nuclear" and "Coulomb" in comparison to the complete calculation "Total".

For both, proton as well as α scattering, the nuclear part is dominant for the excitation of the low-energy part of the PDR and yields large cross sections. This signature is related to transition densities with a strong neutron contribution on the surface whereas in the inner regions protons and neutrons are in phase, a structure that is usually associated with the isoscalar nature of the PDR. While this combination of transition densities leads to large cross sections in the nuclear component, it results in rather small B(E1) values and consequently small Coulomb excitation cross sections.

At higher energies the common structure changes towards more isovector components and, thus, larger Coulomb contributions. The amplitudes due to the Coulomb- and NN-terms become rather close in value and the interference effects between them begin to play an important role. It is interesting to note that even though the transition densities of individual states partly seem to look very different, they share the above-described common underlying features, which result in similar cross sections and this common energy dependence in the response function.

Fig. 2 summarizes the results of all experiments (left column) and the QPM calculation (right column) for ^{140}Ce. Besides the total cross sections for α, proton and photon scattering mentioned so far also the averaged decay branching ratio to the first-excited 2_1^+ state is shown in Fig. 2d as presented in [28]. Each row in Fig. 2 represents the comparison of experimental results with the QPM calculation with respect to a different observable, each of which is sensitive to different aspects of the wave function. The α scattering cross section is sensitive to the isoscalar component of the excited states and is enhanced by surface contributions. Therefore, the large (α, α') cross section for the lower lying group of 1^- states can be identified as a signature of oscillating excess neutrons at the surface of the nucleus [42]. For protons this selectivity is less distinct as inelastic proton scattering is also sensitive to

isovector components and the surface peaked interaction is less pronounced. Compared to α scattering the excitation cross sections for the single excitations are smaller by a factor of about 10, which is well reproduced by the QPM. Photons, on the other hand, are in the case of E1 transitions sensitive to the isovector part and interact with the nucleus as a whole. The large cross sections in the QPM calculation for states around and above 7 MeV compared to the 5–6 MeV region show the increased isovector character of these excitations, forming a transitional region towards the IVGDR at higher energies. The decay intensity of the involved 1^- states to the first-excited 2_1^+ state is connected to the mixing of the PDR built on the ground state to the PDR built on the first-excited state [$2_1^+\times$ PDR] and, thus, allows for a sensitive test of the degree of mixing [28].

The overall agreement between the experimental data and QPM calculations on an absolute scale for all observables simultaneously is satisfactory and first corroborates the present interpretation of the PDR on all its major aspects in a quantitative way. Since each observable is sensitive to a different aspect of the wave function of the excited states, this proves the high accuracy in the detailed modelling of the PDR within the QPM.

In conclusion we have reported on first $(p, p'\gamma)$ experiment to study the PDR in ^{140}Ce, which extends the investigation of the PDR using multiple complementary probes and observables. The presented data set on the PDR in ^{140}Ce is probably the most versatile currently available. In addition, QPM calculations have been performed and combined with state-of-the-art reaction models in order to calculate cross sections, B(E1) values as well as branching ratios in order to compare to the experimental data on an absolute level. For this, the corresponding values have been computed for the first time for each excited 1^- state of the QPM. The overall agreement in order of magnitude and excitation-energy dependence for all observables at the same time proves the accurate modelling of the PDR within the QPM and corroborates the major aspects of the PDR. Further experiments have been performed recently to extend the same multi-messenger investigation of the PDR to other nuclei in different mass regions of the nuclear chart. The results of these experiments together with the ongoing development of microscopic nuclear models will provide an even better understanding of the PDR and its underlying structure.

This work was supported by the Alliance Program of the Helmholtz Association (HA216/EMMI), the Deutsche Forschungsgemeinschaft under Grant Nos. SFB 1245 and ZI 510/7-1 and by the European Commission within the Seventh Framework Programme through IA-ENSAR (contract No. RII3-CT-2010-262010). We further acknowledge the support of S. Brandenburg and the accelerator staff at KVI during the beam time.

References

[1] B.P. Abbott, et al., Astrophys. J. Lett. 848 (2017) L12.
[2] D. Savran, T. Aumann, A. Zilges, Prog. Part. Nucl. Phys. 70 (2013) 210.
[3] A. Bracco, F.C.L. Crespi, E.G. Lanza, Eur. Phys. J. A 51 (2015) 99.
[4] S. Goriely, E. Khan, M. Samyn, Nucl. Phys. A 739 (2004) 331.
[5] E. Litvinova, P. Ring, V. Tselyaev, K. Langanke, Phys. Rev. C 79 (2009) 054312.
[6] I. Daoutidis, S. Goriely, Phys. Rev. C 86 (2012) 034328.
[7] A. Tonchev, N. Tsoneva, C. Bhatia, C. Arnold, S. Goriely, S. Hammond, J. Kelley, E. Kwan, H. Lenske, J. Piekarewicz, et al., Phys. Lett. B 773 (2017) 20.
[8] A. Koning, in: Nuclear Data for Science and Technology, EDP Sciences, 2008.
[9] M. Herman, R. Capote, B. Carlson, P. Obložinský, M. Sin, A. Trkov, H. Wienke, V. Zerkin, Nucl. Data Sheets 108 (2007) 2655.
[10] F. Sokolov, K. Fukuda, H.P. Nawada, IAEA-Tecdoc 1450 (2005).
[11] International Atomic Energy Agency, Fission Product Yield Data for the Transmutation of Minor Actinide Nuclear Waste, 2008.
[12] M. Salvatores, G. Palmiotti, Prog. Part. Nucl. Phys. 66 (2011) 144.
[13] P.-G. Reinhard, W. Nazarewicz, Phys. Rev. C 81 (2010) 051303.
[14] J. Piekarewicz, Phys. Rev. C 83 (2011) 034319.
[15] X. Roca-Maza, X. Vinas, M. Centelles, B.K. Agrawal, G. Colo, N. Paar, J. Piekarewicz, D. Vretenar, Phys. Rev. C 92 (2015) 064304.
[16] M. Baldo, G. Burgio, Prog. Part. Nucl. Phys. 91 (2016) 203.
[17] J.M. Lattimer, Annu. Rev. Nucl. Part. Sci. 62 (2012) 485.
[18] K. Hebeler, J.M. Lattimer, C.J. Pethick, A. Schwenk, Astrophys. J. 773 (2013) 11.
[19] V.G. Soloviev, Theory of Atomic Nuclei: Quasiparticles and Phonons, Institute of Physics, Bristol, 1992.
[20] D. Savran, M. Fritzsche, J. Hasper, K. Lindenberg, S. Müller, V.Y. Ponomarev, K. Sonnabend, A. Zilges, Phys. Rev. Lett. 100 (2008) 232501.
[21] D. Savran, M. Elvers, J. Endres, M. Fritzsche, B. Löher, N. Pietralla, V.Yu. Ponomarev, C. Romig, L. Schnorrenberger, K. Sonnabend, et al., Phys. Rev. C 84 (2011) 024326.
[22] R.-D. Herzberg, P. von Brentano, J. Eberth, J. Enders, R. Fischer, N. Huxel, T. Klemme, P. von Neumann-Cosel, N. Nicolay, N. Pietralla, et al., Phys. Lett. B 390 (1997) 49.
[23] A. Zilges, S. Volz, M. Babilon, T. Hartmann, P. Mohr, K. Vogt, Phys. Lett. B 542 (2002) 43.
[24] A.P. Tonchev, S.L. Hammond, J.H. Kelley, E. Kwan, H. Lenske, G. Rusev, W. Tornow, N. Tsoneva, Phys. Rev. Lett. 104 (2010) 072501.
[25] R. Schwengner, R. Massarczyk, G. Rusev, N. Tsoneva, D. Bemmerer, R. Beyer, R. Hannaske, A.R. Junghans, J.H. Kelley, E. Kwan, et al., Phys. Rev. C 87 (2013) 024306.
[26] J. Isaak, D. Savran, M. Krticka, M.W. Ahmed, J. Beller, E. Fiori, J. Glorius, J.H. Kelley, B. Löher, N. Pietralla, et al., Phys. Lett. B 727 (2013) 361.
[27] R. Massarczyk, R. Schwengner, F. Dönau, S. Frauendorf, M. Anders, D. Bemmerer, R. Beyer, C. Bhatia, E. Birgersson, M. Butterling, et al., Phys. Rev. Lett. 112 (2014) 072501.
[28] B. Löher, D. Savran, T. Aumann, J. Beller, M. Bhike, N. Cooper, V. Derya, M. Duchene, J. Endres, A. Hennig, et al., Phys. Lett. B 756 (2016) 72.
[29] T. Shizuma, T. Hayakawa, I. Daito, H. Ohgaki, S. Miyamoto, F. Minato, Phys. Rev. C 96 (2017) 044316.
[30] A. Tamii, I. Poltoratska, P. von Neumann-Cosel, Y. Fujita, T. Adachi, C.A. Bertulani, J. Carter, M. Dozono, H. Fujita, K. Fujita, et al., Phys. Rev. Lett. 107 (2011) 062502.
[31] C. Iwamoto, H. Utsunomiya, A. Tamii, H. Akimune, H. Nakada, T. Shima, T. Yamagata, T. Kawabata, Y. Fujita, H. Matsubara, et al., Phys. Rev. Lett. 108 (2012) 262501.
[32] A. Krumbholz, P. von Neumann-Cosel, T. Hashimoto, A. Tamii, T. Adachi, C. Bertulani, H. Fujita, Y. Fujita, E. Ganioglu, K. Hatanaka, et al., Phys. Lett. B 744 (2015) 7.
[33] P. Adrich, A. Klimkiewicz, M. Fallot, K. Boretzky, T. Aumann, D. Cortina-Gil, U. Datta Pramanik, Th.W. Elze, H. Emling, H. Geissel, et al., Phys. Rev. Lett. 95 (2005) 132501.
[34] O. Wieland, A. Bracco, F. Camera, G. Benzoni, N. Blasi, S. Brambilla, F.C.L. Crespi, S. Leoni, B. Million, R. Nicolini, et al., Phys. Rev. Lett. 102 (2009) 092502.
[35] D.M. Rossi, P. Adrich, F. Aksouh, H. Alvarez-Pol, T. Aumann, J. Benlliure, M. Böhmer, K. Boretzky, E. Casarejos, M. Chartier, et al., Phys. Rev. Lett. 111 (2013) 242503.
[36] D. Savran, M. Babilon, A.M. van den Berg, M.N. Harakeh, J. Hasper, A. Matic, H.J. Wörtche, A. Zilges, Phys. Rev. Lett. 97 (2006) 172502.
[37] J. Endres, D. Savran, A.M. van den Berg, P. Dendooven, M. Fritzsche, M.N. Harakeh, J. Hasper, H.J. Wörtche, A. Zilges, Phys. Rev. C 80 (2009) 034302.
[38] J. Endres, E. Litvinova, D. Savran, P.A. Butler, M.N. Harakeh, S. Harissopulos, R.-D. Herzberg, R. Krücken, A. Lagoyannis, N. Pietralla, et al., Phys. Rev. Lett. 105 (2010) 212503.
[39] J. Endres, D. Savran, P.A. Butler, M.N. Harakeh, S. Harissopulos, R.-D. Herzberg, R. Krücken, A. Lagoyannis, E. Litvinova, N. Pietralla, et al., Phys. Rev. C 85 (2012) 064331.
[40] V. Derya, J. Endres, M. Elvers, M. Harakeh, N. Pietralla, C. Romig, D. Savran, M. Scheck, F. Siebenhühner, V. Stoica, et al., Nucl. Phys. 906 (2013) 94.
[41] V. Derya, D. Savran, J. Endres, M.N. Harakeh, H. Hergert, J.H. Kelley, P. Papakonstantinou, N. Pietralla, V.Y. Ponomarev, R. Roth, et al., Phys. Lett. B 730 (2014) 288.
[42] E.G. Lanza, A. Vitturi, E. Litvinova, D. Savran, Phys. Rev. C 89 (2014) 041601.
[43] L. Pellegri, A. Bracco, F. Crespi, S. Leoni, F. Camera, E. Lanza, M. Kmiecik, A. Maj, R. Avigo, G. Benzoni, et al., Phys. Lett. B 738 (2014) 519.
[44] F.C.L. Crespi, A. Bracco, R. Nicolini, D. Mengoni, L. Pellegri, E.G. Lanza, S. Leoni, A. Maj, M. Kmiecik, R. Avigo, et al., Phys. Rev. Lett. 113 (2014) 012501.
[45] F.C.L. Crespi, A. Bracco, R. Nicolini, E.G. Lanza, A. Vitturi, D. Mengoni, S. Leoni, G. Benzoni, N. Blasi, C. Boiano, et al., Phys. Rev. C 91 (2015) 024323.
[46] M. Krzysiek, M. Kmiecik, A. Maj, P. Bednarczyk, A. Bracco, F.C.L. Crespi, E.G. Lanza, E. Litvinova, N. Paar, R. Avigo, et al., Phys. Rev. C 93 (2016) 044330.
[47] A.M. van den Berg, Nucl. Instrum. Methods Phys. Res., Sect. B 99 (1995) 637.
[48] B.A.M. Krüsemann, R. Bassini, F. Ellinghaus, D. Frekers, M. Hagemann, V.M. Hannen, H. von Heynitz, J. Heyse, S. Rakers, H. Sohlbach, et al., Nucl. Instrum. Methods Phys. Res., Sect. A 431 (1999) 236.
[49] D. Savran, A.M. van den Berg, M.N. Harakeh, K. Ramspeck, H.J. Wörtche, A. Zilges, Nucl. Instrum. Methods Phys. Res., Sect. A 564 (2006) 267.
[50] M.A. Büssing, M. Elvers, J. Endres, J. Hasper, A. Zilges, M. Fritzsche, K. Lindenberg, S. Müller, D. Savran, K. Sonnabend, Phys. Rev. C 78 (2008) 044309.
[51] B. Löher, PhD thesis, University Mainz, 2014, http://ubm.opus.hbz-nrw.de/volltexte/2014/3819/.

[52] S. Volz, N. Tsoneva, M. Babilon, M. Elvers, J. Hasper, R.-D. Herzberg, H. Lenske, K. Lindenberg, D. Savran, A. Zilges, Nucl. Phys. A 779 (2006) 1.
[53] C. Romig, D. Savran, J. Beller, J. Birkhan, A. Endres, M. Fritzsche, J. Glorius, J. Isaak, N. Pietralla, M. Scheck, et al., Phys. Lett. B 744 (2015) 369.
[54] J. Raynal, Program DWBA07, NEA Data Service NEA1209/08.
[55] W.G. Love, M.A. Franey, Phys. Rev. C 24 (1981) 1073.
[56] M.A. Franey, W.G. Love, Phys. Rev. C 31 (1985) 488.
[57] E.G. Lanza, F. Catara, D. Gambacurta, M.V. Andrés, P. Chomaz, Phys. Rev. C 79 (2009) 054615.
[58] E.G. Lanza, A. Vitturi, M.V. Andrés, F. Catara, D. Gambacurta, Phys. Rev. C 84 (2011) 064602.
[59] E.G. Lanza, A. Vitturi, M.V. Andrés, Phys. Rev. C 91 (2015) 054607.
[60] G. Bertsch, J. Borysowicz, H. McManus, W.G. Love, Nucl. Phys. A 284 (1977) 399.
[61] G.R. Satchler, W.G. Love, Phys. Rep. 55 (1979) 183.